Sensors and Materials, Vol. 34, No. 4 (2022) 1389–1400
MYU Tokyo

S & M 2898

Application of Supercapacitor to Photovoltaic Module for Power Generation Compensation

Hung-Cheng Chen,[1] Shin-Shiuan Li,[1] Shing-Lih Wu,[2*] and Chin-Yu Hung[3]

[1]Prospective Technology of Electrical Engineering and Computer Science, National Chin-Yi University of Technology, No. 57, Sec. 2, Zhongshan Rd., Taiping Dist., Taichung 411030, Taiwan
[2]Department of Electrical Engineering, National Taitung Junior College, No. 889, Jhengci N. Rd., Taitung 95045, Taiwan
[3]Department of Electrical Engineering, National Chin-Yi University of Technology, No. 57, Sec. 2, Zhongshan Rd., Taiping Dist., Taichung 411030, Taiwan

(Received September 6, 2021; accepted January 19, 2022)

Keywords: photovoltaic module, supercapacitor, shade compensation

The current–voltage characteristic of a photovoltaic module shows a nonlinear relationship, and the photovoltaic module has one optimal operation point. However, photovoltaic modules are affected by clouds and dust, resulting in reduced output power generation and reduced quality and stability of the power supply due to the interrupted operation of the converter. To solve this problem, we propose the application of a supercapacitor that stores and releases electric energy to compensate for the energy shortage of the photovoltaic power generation system in shade. To test the photovoltaic module with the supercapacitor, we designed an experimental platform with a self-designed pyrheliometer to measure the luminous intensity. The experimental platform controlled the photovoltaic module by using the supercapacitor to compensate for the decreased power due to clouds and dust. The result indicated that the use of the supercapacitor enabled a constant power supply at the same workload. The comparison of the power supply with and without the supercapacitor under full (100%) and partial shade (20%) showed that the voltage of the photovoltaic module was effectively compensated to prevent system shutdown caused by an instantaneous voltage drop.

1. Introduction

The continuous development of science and technology has increased energy demand rapidly, while supplies of fossil fuels are limited and their prices are rising. Fossil fuel use and its exploitation are a considerable burden on the environment and directly related to climate change.[1–5] As a renewable energy, solar energy is regarded as ideal for sustainable development with low pollution and a low maintenance cost.[6–10] The current–voltage (I–V) relationship of a photovoltaic module is nonlinear, and the photovoltaic module has one optimal operating point.[11–16] Photovoltaic modules are affected by clouds and dust, which reduce power generation and the quality and stability of the power supply.[17–24] To solve this problem, Silvestre *et al.* proposed a photovoltaic module with bypass diodes to prevent damage due to a reverse

*Corresponding author: e-mail: lihchoug@ntc.edu.tw
https://doi.org/10.18494/SAM3649

ISSN 0914-4935

voltage.[25] The bypass diode protects the photovoltaic array, which effectively improves the power output.

As there has been little attempt to use a supercapacitor for a photovoltaic module, the application of a supercapacitor to compensate for a photovoltaic module in shade and a control strategy for the system are proposed in this study. We analyze the performance of the system with a supercapacitor and verify its feasibility. The experimental results show that the experimental platform with a supercapacitor compensates for the generated power of the photovoltaic module in shade.

2. System and Experiments

2.1 Detection circuit of maximum power point

We present the application of a supercapacitor for the power compensation of a photovoltaic module in shade. As a photovoltaic module ideally operates at the maximum power point (MPP), where a photovoltaic module produces its highest possible voltage, a controllable MPP detection circuit is designed as shown in Fig. 1. The output power of the photovoltaic module is connected to a workload (electrical resistance), and the circuit is connected to a series of current meters and a voltage meter. Halogen lamps are used as the light source for the photovoltaic module. When the photovoltaic module is illuminated, its output voltage and current are monitored. At the same time, the voltage and current of the workload are measured and compared with the output voltage and current of the photovoltaic module to determine whether the MPP is reached. Then, the resistance of the workload is adjusted to find the MPP. A flow chart for determining the MPP is shown in Fig. 2.

2.2 Platform architecture and experimental process

The supercapacitor used to compensate the power generation of a photovoltaic module in shade is included in an experimental platform with a photovoltaic module, a self-designed pyrheliometer, a controller, a charger, a supercapacitor, a recorder, switches, and a workload, as shown in Fig. 3. In the self-designed pyrheliometer, a small silicon solar cell senses solar

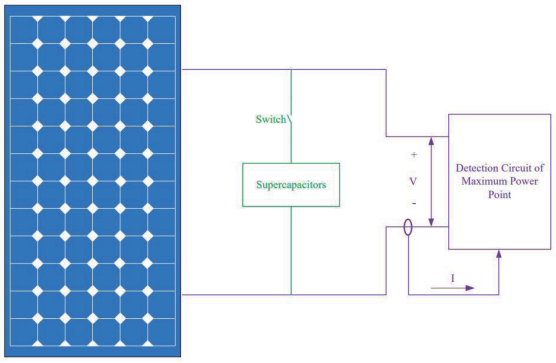

Fig. 1. (Color online) Schematic diagram of the circuit for detecting the MPP.

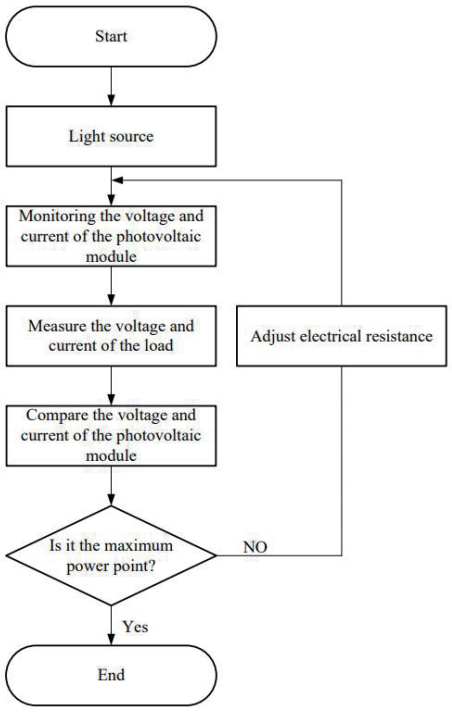

Fig. 2. Flow chart for determining the electrical resistance of the MPP.

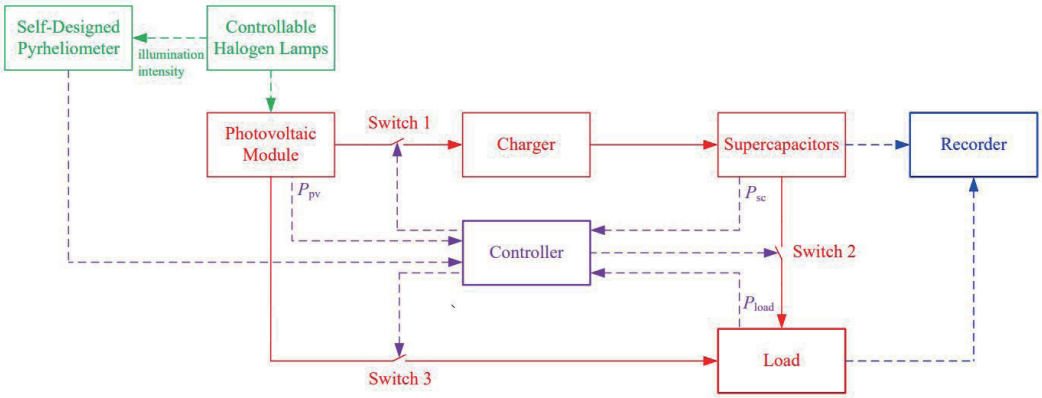

Fig. 3. (Color online) Schematic diagram of experimental platform architecture.

radiation and measures the short-circuit current of the cell. It converts its current signal into a voltage signal to obtain the luminous intensity. The self-designed pyrheliometer is mainly used to measure and monitor the luminous intensity of the photovoltaic module and send the data to the controller.

Figure 4 shows the layout of the halogen lamps used for luminous intensity measurement in the experiment. We used four 150 W and nine 50 W halogen lamps as the light source to illuminate 13 locations. An acrylic plate was used to simulate different degrees of shade to measure how shade affects the luminous intensity of the photovoltaic module.

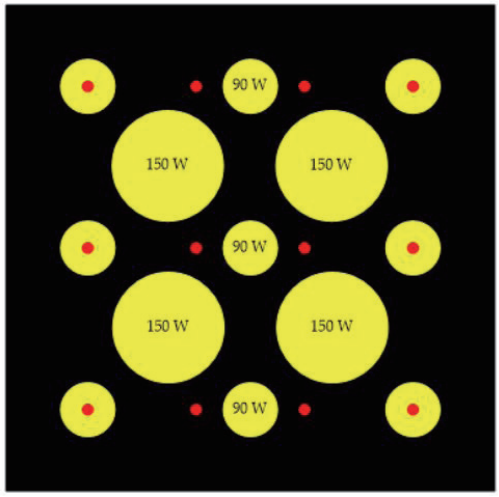

Fig. 4. (Color online) Layout of controllable halogen lamps for luminous intensity measurement.

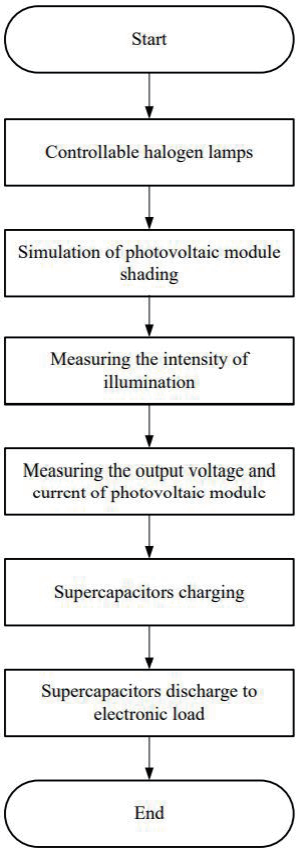

Fig. 5. Flow chart of the experimental process.

In the experiment, the luminous intensity of the photovoltaic module and the voltage and charging current of the supercapacitor were measured. At the same time, the amount of charged electricity was measured. Finally, the supercapacitor discharged the stored power to the workload, and the discharged power was measured. Figure 5 shows a flow chart of the experimental process.

2.3 Self-designed pyrheliometer

To determine the luminous intensity, the relationship between the output current of the solar cell and the luminous intensity must be understood, as shown in Fig. 6. The output current of the solar cell is proportional to the incident luminous intensity. The stronger the light, the higher the output power of the solar cell. With the decrease in luminous intensity, the shape of the *I*–*V* curve remains unchanged and the short-circuit current decreases gradually. The small change in the open-circuit voltage with the luminous intensity is because the solar cell directly converts solar radiant energy into electrical energy. Therefore, we use the self-designed pyrheliometer to measure the short-circuit current of the solar cell and convert the current signal into a voltage signal by using a programmable logic controller (PLC). The luminous intensity is calculated

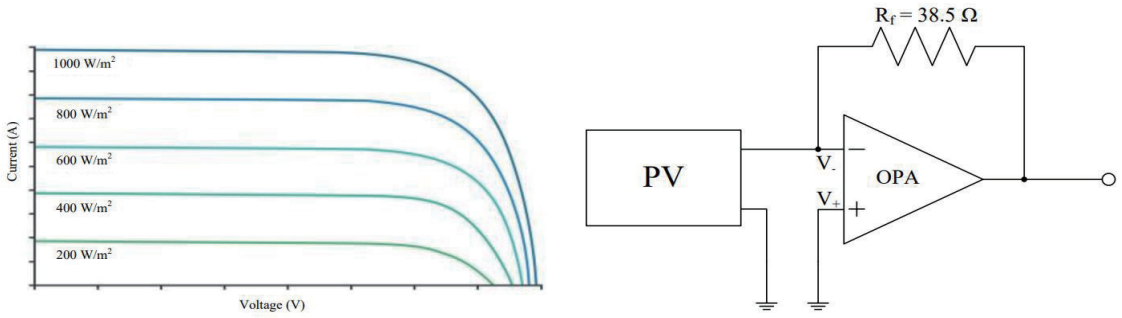

Fig. 6. (Color online) Self-designed pyrheliometer: (a) *I–V* curve of solar cell and (b) detection circuit.

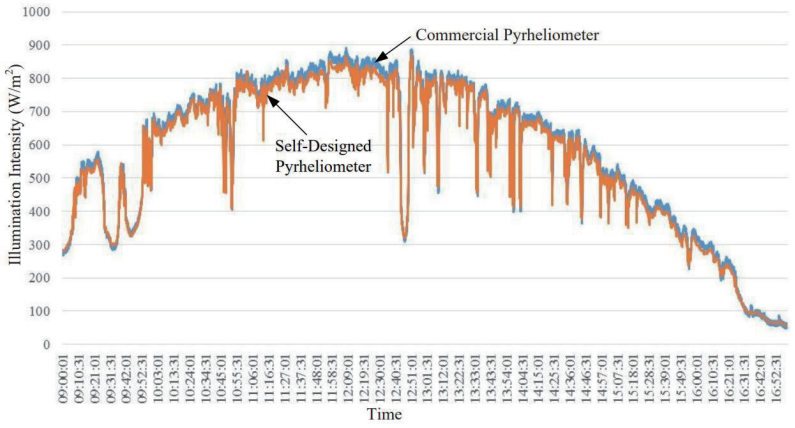

Fig. 7. (Color online) Difference in luminous intensity measured by commercial and self-designed pyrheliometers.

from the potential difference of the generated power. The pyrheliometer collects the luminous intensity data during the experiment and sends the data to the controller. The accuracy of the pyrheliometer is compared with that of a commercial pyrheliometer. The degree of shade changes the luminous intensity significantly. The commercial pyrheliometer showed 3.6% higher intensity than the proposed pyrheliometer. Figure 7 shows a dramatic fluctuation in luminous intensity. In the presence of cloudd, the luminous intensity measured by the commercial pyrheliometer decreases by 8%. Figure 8 shows the measurements obtained during a period of 16 h and indicates that the difference in the luminous intensity above 200 W/m^2 for the commercial and self-designed pyrheliometer is within 4%, whereas the difference is larger between 100 and 200 W/m^2.

2.4 Control strategy

In a supercapacitor, the controller receives the signals of luminous intensity, P_{pv}, P_{load}, and P_{sc}. The control strategy is decided by comparing the signals. The control strategy and switch arrangement are shown in Table 1. The signal obtained by the pyrheliometer is mainly used to monitor the luminous intensity of the photovoltaic module and is stored in the controller.

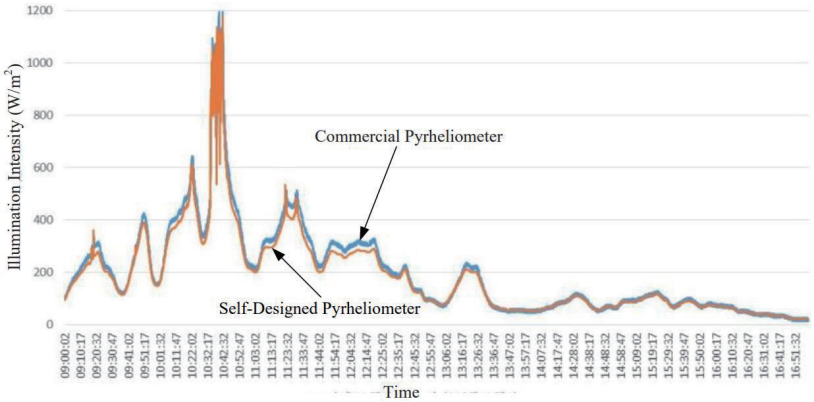

Fig. 8. (Color online) Difference in luminous intensity measured in shade by commercial and self-designed pyrheliometers.

Table 1
Control strategy and switch arrangement.

Control strategy	Judgment mode	Switch 1	Switch 2	Switch 3
1	$P_{pv} > P_{load}$	ON	ON	ON
2	$P_{pv} > P_{load}$	OFF	ON	
3	$P_{pv} > P_{load}$	ON	OFF	
4	$P_{pv} = P_{load}$	OFF	OFF	
5	$P_{pv} < P_{load}$ but $P_{sc} > P_{load}$	ON	ON	OFF
6	$P_{pv} < P_{load}$ but $P_{sc} > P_{load}$	OFF	ON	
7	$P_{pv} < P_{load}$, $P_{sc} < P_{load}$ and $P_{pv} > P_{sc}$	ON	OFF	
8	$P_{pv} < P_{load}$, $P_{sc} < P_{load}$ and $P_{pv} < P_{sc}$	OFF	OFF	

- **Control strategy 1**: When the photovoltaic module generates power (P_{pv}) and the controller judges $P_{pv} > P_{load}$, switch 3 is switched on to transfer sufficient power to the workload, thus supplying excess power. When the supercapacitor is not fully charged, switch 1 is switched on to transfer the remaining power ($P_{pv} - P_{load}$) to the supercapacitor for charging. At this time, although the supercapacitor is not fully charged, insufficient power for the workload is avoided in partial shade with switch 2 on.
- **Control strategy 2**: When the photovoltaic module generates power (P_{pv}) and the controller judges $P_{pv} > P_{load}$, switch 3 is switched on to transfer sufficient power to the workload. The supercapacitor is fully charged and switch 1 is switched off. At this time, switch 2 is switched on to avoid insufficient power for the workload in partial shade.
- **Control strategy 3**: When the photovoltaic module generates power (P_{pv}) and the controller judges $P_{pv} > P_{load}$, switch 3 is switched on to transfer sufficient power to the workload as excess power. When the supercapacitor is not fully charged, switch 1 is switched on to

transfer the remaining power ($P_{pv} - P_{load}$) for charging. At this time, since the initial state of the supercapacitor is without power, switch 2 is switched off.

- Control strategy 4: When the photovoltaic module generates power (P_{pv}) and the controller judges $P_{pv} = P_{load}$, switch 3 is switched on to transfer sufficient power to the workload. However, the power is only enough to supply the workload, so switches 1 and 2 are switched off.
- **Control strategy 5**: When the photovoltaic module generates power (P_{pv}) and the controller judges $P_{pv} < P_{load}$, switch 3 is switched off. If the controller judges that the power of the supercapacitor ($P_{sc} > P_{load}$) is sufficient to supply the workload, switch 2 is switched on and the supercapacitor maintains the workload. At this time, although the power of the photovoltaic module is insufficient to supply the workload, it is sufficient to supply the partially charged supercapacitor, so switch 1 is switched on.
- **Control strategy 6**: When the photovoltaic module generates power (P_{pv}) and the controller judges $P_{pv} < P_{load}$, switch 3 is switched off. If the controller judges that the power of the supercapacitor ($P_{sc} > P_{load}$) is sufficient to supply the workload, switch 2 is switched on and the supercapacitor is maintained to operate the workload. At this time, since the initial state of the supercapacitor is fully charged, switch 1 is switched off.
- **Control strategy 7**: When the photovoltaic module generates power (P_{pv}) and the controller judges $P_{pv} < P_{load}$ and $P_{sc} < P_{load}$, switches 2 and 3 are switched off. If the controller judges $P_{pv} > P_{sc}$, switch 1 is switched on and the photovoltaic module charges the supercapacitor. However, this is the least effective control strategy.
- **Control strategy 8**: When the photovoltaic module generates power (P_{pv}) and the controller judges $P_{pv} < P_{load}$, $P_{pv} < P_{sc}$, and $P_{sc} < P_{load}$, switches 1, 2, and 3 are switched off, indicating that the photovoltaic module and supercapacitor have no power to supply the workload, so the system is shut down.

3. Results and Discussion

The power is measured in two cases: with and without the supercapacitor. First, the MPP of the photovoltaic module must be found. The MPP circuit is verified for a resistance of 30 Ω by considering the *I–V* relationship of the light source (halogen lamps) of the photovoltaic module, as shown in Fig. 9.

The luminous intensity of the halogen lamps used as the light source is measured by the pyrheliometer in two degrees of shade, where the shade is simulated by switching off several lamps. First, to simulate the sunshine, all lamps are switched on, and the output voltage and current of the photovoltaic module are measured. When the workload voltage becomes stable, several lamps are switched off to simulate shade. The voltage and current are measured with full shade (with all lamps switched off) and partial shade (20% of the highest luminous intensity with several lamps switched off). The voltage and current are recorded for 120 s. Then, the generated power of the photovoltaic module is calculated. This experiment is carried out with and without the supercapacitor.

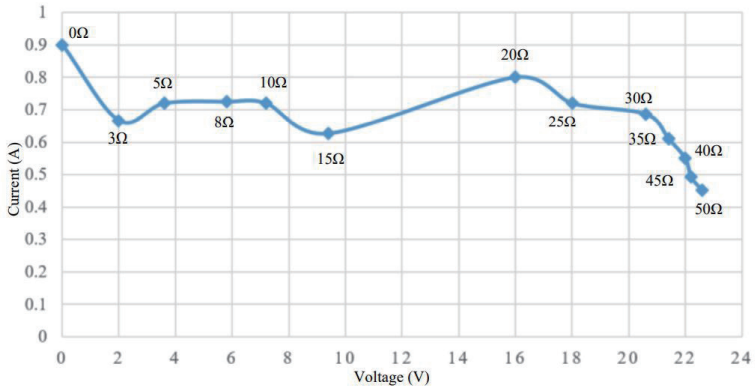

Fig. 9. (Color online) *I–V* characteristic curve of the photovoltaic module.

3.1 Measurements without supercapacitor

In full shade, the voltage and current from the photovoltaic module are less than those without shade. Figure 10 shows the voltage and current in full shade (100%) without the supercapacitor. The measurement data shows that the voltage and current respectively drop from 22.0 V and 736 mA to 0 during the 120 s of shade. The electric charge in full shade is also reduced from 88.32 C to 0.

For the partial shade of 20%, one 150 W and two 90 W halogen lamps are switched off. Then, the voltage and current are measured as shown in Fig. 11.

The voltage and current respectively decrease to 16.6 V and 592 mA during the 120 s of shade. The electric charge in partial shade is reduced to 17.28 C. Table 2 shows the measurement data of voltage and current for the two different levels of shade.

3.2 Measurements with supercapacitor

When using the supercapacitor, the following three different strategies are applied to the photovoltaic module.

(1) $t < t_0$

When $t < t_0$, the photovoltaic module generates enough power to charge the supercapacitor, so control strategy 1 is applied.

(2) $t_0 \leq t \leq t_1$

When $t = t_0$, the supercapacitor is charged fully to 20.0 V and 40 mA, which requires control strategy 2. When $t_0 < t \leq t_1$, the photovoltaic module is in partial shade, so the supercapacitor discharges to the workload according to control strategy 6, causing its voltage and current to decrease from 20.0 to 8.0 V and from 944 to 280 mA, respectively. The discharge time is 120 s.

(3) $t > t_1$

When $t > t_1$, the photovoltaic module is no longer in shade and returns to normal operation. Thus, the supercapacitor is charged and control strategy 1 is applied. When the supercapacitor is fully charged, the electric charges of the photovoltaic module and supercapacitor are −3.2 and

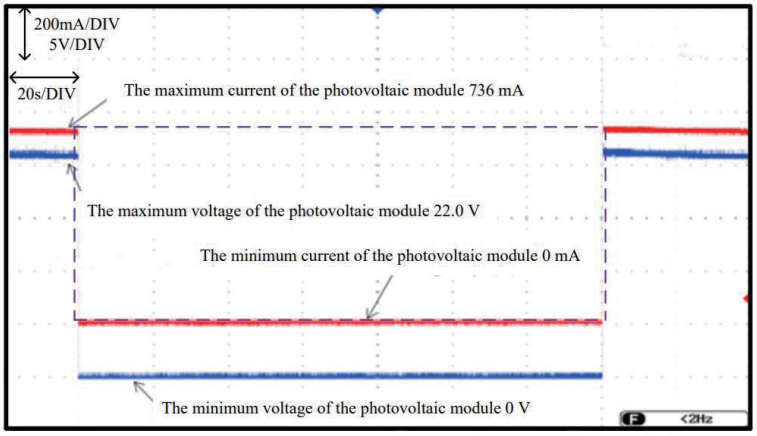

Fig. 10. (Color online) Voltage and current in full shade without supercapacitor.

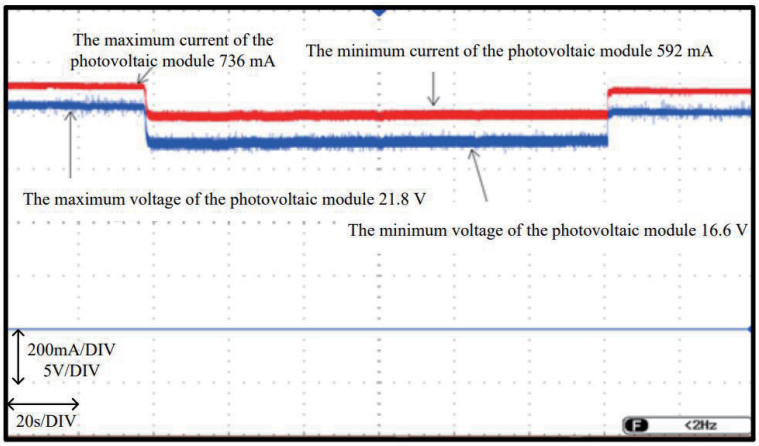

Fig. 11. (Color online) Voltage and current in partial shade (20%) without supercapacitor.

Table 2
Measurement results of voltage, current, and electric charge in full and partial shade without supercapacitor.

Situation	Full shade (100%)	Partial shade (20%)
Voltage (V)	0	16.6
Current (mA)	0	592
Electic charge (C)	0	17.28
Shade time (s)	120	

68 C, respectively, while the total electric charge of the workload is 64.8 C. The measured voltages and currents under the different strategies are shown in Fig. 12. Figure 13 shows the voltage and current of the photovoltaic module with the supercapacitor in partial shade. Table 3 presents the measurement results of the voltage, current, and electric charge of the photovoltaic module with the supercapacitor. The results indicate that the supercapacitor supplies power to the workload when the solar cell does not generate enough power. Even in full shade, the supercapacitor discharges power for 120 s without interruption. In partial shade, the

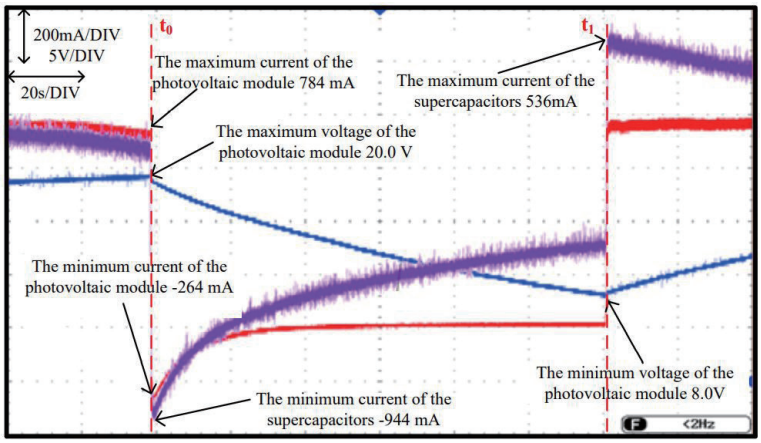

Fig. 12. (Color online) Voltage and current in full shade (100%) with supercapacitor.

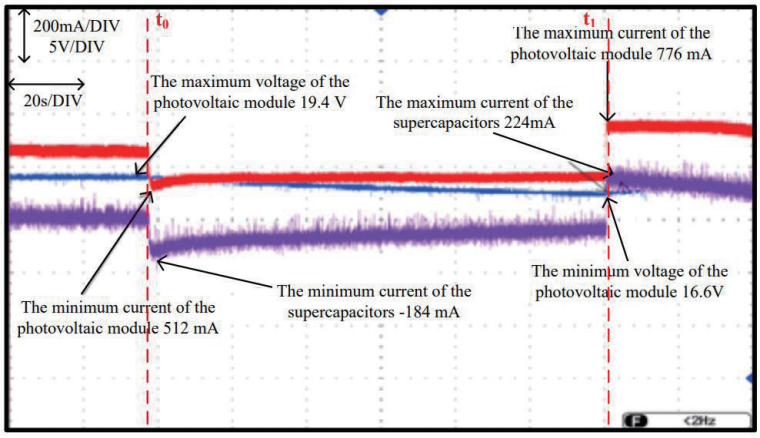

Fig. 13. (Color online) Voltage and current in partial shade (20%) with supercapacitor.

Table 3
Measurement results of voltage, current, and electric charge in full and partial shade with supercapacitor.

Situation	Full shade (100%)	Partial shade (20%)
Photovoltaic module voltage (V)	20.0→8.0	19.4→16.6
Electric charge of photovoltaic module (C)	−3.2	64.8
Electric charge compensated by supercapacitor (C)	68	9.6
Total electric charge supplied to workload (C)	64.8	74.4
Shade time (s)	120	

supercapacitor supplies power while it is charged as it provides 9.6 C to compensate for the electric charge of the photovoltaic module.

The supercapacitor supplies the same power to the workload by compensating for the photovoltaic module in shade. The electric charge is supplied by the supercapacitor without light incidence. Comparison of the measured data with and without the supercapacitor reveals that enough power is supplied from it even without any power generation from the photovoltaic module (Table 4).

Table 4
Summary of experimental results in this study.

Situation	Full shade (100%)	Partial shade (20%)
Required electric charge (C)	88.32	
Voltage of photovoltaic module without supercapacitor (V)	0	16.6
Electric charge supplied to workload without supercapacitor (C)	0	71.04
Voltage of photovoltaic module with supercapacitor (V)	20.0→8.0	19.4→16.6
Electric charge supplied to workload with supercapacitor (C)	64.8	74.4
Shade time (s)	120	

4. Conclusions

A supercapacitor is applied to a photovoltaic module to compensate for its insufficient power generation in the shade, which hinders it from generating enough power for a connected workload. During 120 s of full shade, the voltage and current of the photovoltaic module without a supercapacitor drop from 20 V and 71.04 mA, respectively, to 0. In partial shade (20%), the voltage of the photovoltaic module decreases from 19.4 to 16.6 V and the electric charge provided by the supercapacitor is 64.8 C. When the shade is 20%, the electric charge provided by the supercapacitor is 74.4 C. When 88.32 C of the electric charge is supplied to the workload that is connected to the photovoltaic module, the supercapacitor provides compensation of 68 and 9.6 C in full shade and partial shade, respectively. The results show that the supercapacitor prevents system shutdown caused by the instantaneous voltage drop of the photovoltaic module in the shade. This demonstrates the efficiency of the supercapacitor for the photovoltaic module in the shade to improve the voltage stability and to enhance the sustainability and quality of the power supply.

Acknowledgments

This research was partially supported by the Ministry of Science and Technology of Taiwan under Grant MOST 109-2622-E-167-016.

References

1 M. Z. S. El-Dein, M. Kazerani, and M. M. A. Salama: IEEE Trans. Sustainable Energy **4** (2013) 145. https://doi.org/10.1109/TSTE.2012.2208128
2 A. Y. Saber and G. K. Venayagamoorthy: IEEE Trans. Ind. Electron. **58** (2011) 1229. https://doi.org/10.1109/TIE.2010.2047828
3 H. M. Hasanien: IEEE Trans. Sustainable Energy **6** (2015) 509. https://doi.org/10.1109/TSTE.2015.2389858
4 P. Vithayasrichareon, G. Mills, and I. F. MacGill: IEEE Trans. Sustainable Energy **6** (2015) 899. https://doi.org/10.1109/TSTE.2015.2418338
5 K. Rahbar, C. C.y Chai, and R. Zhang: IEEE Trans. Smart Grid **9** (2018) 1482. https://doi.org/10.1109/TSG.2016.2600863
6 T. Esram and P. L. Chapman: IEEE Trans. Energy Convers. **22** (2007) 439. https://doi.org/10.1109/TEC.2006.874230
7 N. Liu, Q. Chen, X. Lu, J. Liu, and J. Zhang: IEEE Trans. Ind. Electron. **62** (2015) 4878. https://doi.org/10.1109/TIE.2015.2404316

8 G. Velasco-Quesada, F. Guinjoan-Gispert, R. Piqué-López, M. Román-Lumbreras, and A. Conesa-Roca: IEEE Trans. Ind. Electron. **56** (2009) 4319. https://doi.org/10.1109/TIE.2009.2024664
9 W. Mao, X. Zhang, R. Cao, F. Wang, T. Zhao, and L. Xu: IEEE Trans. Ind. Electron. **65** (2018) 2653. https://doi.org/10.1109/TIE.2017.2736483
10 M. B. Shadmand, R. S. Balog, and M. D. Johnson: IEEE Trans. Sustainable Energy **5** (2014) 1434. https://doi.org/10.1109/TSTE.2014.2345745
11 A. Sangwongwanich and F. Blaabjerg: IEEE Trans. Power Electron. **34** (2019) 8279. https://doi.org/10.1109/TPEL.2019.2902880
12 D. Venkatramanan and V. John: IEEE Trans. Ind. Appl. **55** (2019) 6234. https://doi.org/10.1109/TIA.2019.2937856
13 N. Priyadarshi, S. Padmanaban, J. B. Holm-Nielsen, F. Blaabjerg, and M. S. Bhaskar: IEEE Syst. J. **14** (2020) 1218. https://doi.org/10.1109/JSYST.2019.2949083
14 D. S. Pillai and N. Rajasekar: IEEE Trans. Power Electron. **34** (2019) 8646. https://doi.org/10.1109/TPEL.2018.2884292
15 A. Lashab, D. Sera, and J. M. Guerrero: IEEE Trans. Power Electron. **34** (2019) 9686. https://doi.org/10.1109/TPEL.2019.2892809
16 Y. Zhou, C. N. M. Ho, and K. K. Siu: IEEE J. Photovoltaics **9** (2019) 849. https://doi.org/10.1109/JPHOTOV.2019.2899470
17 M. Orkisz: IEEE Trans. Ind. Appl. **54** (2018) 4825. https://doi.org/10.1109/TIA.2018.2841818
18 M. R. Maghami, H. Hizam, C. Gomes, M. A. Radzi, M. I. Rezadad, and S. Hajighorbani: Renewable Sustainable Energy Rev. **59** (2016) 1307. https://doi.org/10.1016/j.rser.2016.01.044
19 A. Maki and S. Valkealahti: IEEE Trans. Energy Convers. **28** (2013) 1008. https://doi.org/10.1109/TEC.2013.2274280
20 R. Ramaprabha and B. L. Mathur: Int. J. Photoenergy **2012** (2012) 120214. https://doi.org/10.1155/2012/120214
21 C. Chen, K. Chen, and Y. Chen: IEEE Trans. Power Electron. **29** (2014) 4723. https://doi.org/10.1109/TPEL.2013.2287752
22 A. Dolara, G. C. Lazaroiu, S. Leva, and G. Manzolini: Energy **55** (2013) 466. https://doi.org/10.1016/j.energy.2013.04.009
23 S. Z. M. Golroodbari, A. C. de Waal, and W. G. J. H. M. van Sark: Energies **11** (2018) 250. https://doi.org/10.3390/en11010250
24 S. I. Serna-Garcés, J. D. Bastidas-Rodríguez, and C. A. Ramos-Paja: Energies **9** (2015) 2. https://doi.org/10.3390/en9010002
25 S. Silvestre, A. Boronat, and A. Chouder: Appl. Energy **86** (2009) 1632. https://doi.org/10.1016/j.apenergy.2009.01.020